

**MIXED OXIDES OF Zn/Al, Zn/Al-La AND Zn-Mg/Al: PREPARATION, CHARACTERIZATION AND PHOTOCATALYTIC ACTIVITY IN DICLOFENAC DEGRADATION**

**ÓXIDOS MIXTOS DE Zn/Al, Zn/Al-La AND Zn-Mg/Al: PREPARACIÓN, CARACTERIZACIÓN Y ACTIVIDAD FOTOCATALITICA EN LA DEGRADACIÓN DEL DICLOFENACO**

J.A. Morales-Zarate, S.P. Paredes-Carrera, L.V. Castro-Sotelo\*

*Escuela Superior de Ingeniería Química e Industrias Extractivas, Instituto Politécnico Nacional, Unidad Profesional "Adolfo López Mateos", Zacatenco, Deleg. Gustavo A. Madero, C.P. 07738, Ciudad de México, México.*

Received: October 20, 2017; Accepted: March 28, 2018

**Abstract**

Layered double hydroxides (hydrotalcites) with Zn/Al, Zn/Al-La and Zn-Mg/Al were synthesized by the coprecipitation method with microwave and ultrasonic hydrothermal aging and nitrate as the interlayer anion; those materials have been used as precursors for the preparation of mixed metal oxides by calcination at 500 °C. The formation of ZnO was detected in the mixed oxides, indicating the destruction of lamellar structure with different degree of crystallinity depending of the hydrothermal method used. All the mixed oxides were tested for the study of degradation of diclofenac (DCF) and TiO<sub>2</sub> as reference. The photocatalysis were investigated in term of UV absorbance for an initial DCF concentration (50 mgL<sup>-1</sup>) in a batch reactor system. All the samples resulted active as heterogenous photocatalysts. These results showed that mixed oxides prepared are promising materials for an effective diclofenac degradation.

*Keywords:* hydrotalcites Zn/Al-La, photocatalysis, diclofenac, LDH, degradation.

**Resumen**

Se sintetizaron hidróxidos dobles laminares (hidrotalcitas) con Zn/Al, Zn/Al-La y Zn-Mg/Al mediante el método de coprecipitación con tratamiento hidrotérmico de envejecimiento de microondas y ultrasonido con anión interlaminares de nitrato; estos materiales se han utilizado como precursores para la preparación de óxidos mixtos metálicos por calcinación a 500 °C. La formación de ZnO se detectó en los óxidos mixtos, lo que indica la destrucción de la estructura laminar con diferente grado de cristalinidad dependiendo del método hidrotérmico utilizado. Todos los óxidos mixtos se probaron para el estudio de la degradación de diclofenaco (DCF) y el TiO<sub>2</sub> como referencia. La fotocatalisis se investigó en términos de absorbancia de UV para una concentración inicial de DCF (50 mgL<sup>-1</sup>) en un sistema de reactor discontinuo. Todas las muestras resultaron activas como fotocatalizadores heterogéneos. Estos resultados mostraron que los óxidos mixtos preparados son materiales prometedores para una degradación efectiva del diclofenaco.

*Palabras clave:* hidrotalcitas Zn/Al-La, fotocatalisis, diclofenaco, CTH, degradación.

**1 Introduction**

Diclofenac sodium salt (DCF), sodium 2-[2-(2, 6-dichlorophenyl) amino]-phenyl] acetate, is a synthetic nonsteroidal anti-inflammatory agent (NSAID) with antipyretic and analgesic action, a drug one of the most frequently detected pharmaceuticals in waters and urban wastewater (Andreozzi *et al.*, 2003) Recent studies show that advanced oxidation processes (AOPs) can be successfully applied for the removal of

pharmaceuticals from water (Klavarioti *et al.*, 2009). One of the most popular photocatalysis for AOPs is the TiO<sub>2</sub> because of its capacity to mineralize organic pollutant, to operate without pH adjustment (Rizzo *et al.*, 2009). Some authors reported that the toxicity of the degradation products increased during the oxidation but at the end of the irradiation tie no toxicity was observed. The oxidation processes could be hydrolysis, dehydration, adduct formation, dimerization, rearrangement, excipient reaction and often from the combination of these processes

\* Corresponding author. E-mail: lcastros@ipn.mx or salikwilly@yahoo.com.mx ,  
Tel/Fax: +52 5557296000 ext. 54229  
doi: 10.24275/uam/izt/dcbi/revmexingquim/2018v17n3/Morales  
issn-e: 2395-8472

(Galmier *et al.*, 2005). For the AOP photocatalytic semiconductor materials are widely used to degrade organic contaminants in water. The photocatalytic process, describe a process in which light is used to activate a catalyst or one substance that modifies the rate of a chemical reaction without being involved itself in the chemical transformation. The most commonly solids used for AOP processes are TiO<sub>2</sub> and ZnO photocatalysts (Rizzo *et al.*, 2009; Tzompantzin *et al.*, 2014; Mahjoubi *et al.*, 2017; Valente *et al.*, 2009; Patzkó *et al.*, 2005; Seftel *et al.*, 2008; Zhang *et al.*, 2016; Zhao *et al.*, 2010). The photocatalytic properties of the ZnO was reported by Patzko *et al.* 2005, they reported ZnAl-layered double hydroxides with various Zn/Al ratios by sol-gel method and the samples were calcinated and studied with aqueous phenol solution. Tzompantzi *et al.* (2014) reported ZnAlLa LDH and their mixed oxides evaluated in the photoactivity in the degradation of phenol using a low intensity UV-Vis showed values in phenol mineralization 88% with the ZnAlLa samples.

The Zn-Al LDHs have many other applications, Mahjoubi *et al.* (2017) synthesized Zn-Al layered double hydroxides intercalated with different interlaminal ions via coprecipitation method at a constant solution pH for methyl orange adsorption.

There are some catalysts used for elimination of phenolic compounds such as Valente *et al.* (2009) prepared five samples of Mg-Zn-Al LDHs by coprecipitation method and the mixed oxides were tested for the photocatalytic degradation of 2,4-D and phenol with nearly 70% of initial 0.42 mmol/L was degraded after 6 h.

LDHs are materials that are simple and economical to synthesize in the laboratory, as reference material TiO<sub>2</sub> was used for the degradation of DCF, Calza *et al.* (2006) and many others authors have been described that the oxidation of DCF takes place by either indirect oxidation by surface bound hydroxyl radicals or directly via the valence band hole.

Some LDHs have been reported recently reported as a good alternative for the photodegradation of organic compounds methyl-orange (Seftel *et al.*, 2008), orange II sodium salt (Zhang *et al.*, 2016), methylene-blue (Parida *et al.*, 2007), methyl-violet (Parida *et al.*, 2012), malachite-green (Parida *et al.*, 2012), acridine orange, Congo red and methyl orange (Khan *et al.* 2016) in aqueous media.

Because hydrotalcite-type compounds are very rare in nature, it is necessary to synthesize them. However, these materials are promising for their ease of synthesis in aqueous solutions from salts of the

cations to be used, in addition to being able to store large number of anions in the interlaminal space, favoring a simple preparation of metal catalysts by means of a simple heat treatment (Cavani *et al.*, 1991). The main disadvantage of this method is the time required to crystallize the hydrotalcite. New synthetic routes have been explored, for instance the sol-gel method (expensive reactants), many authors have been using microwave irradiation for the synthesis of inorganic solids (Bergadá *et al.*, 2007). Climent *et al.* (2004) reported the synthesis of LDH of Mg-Al by different methods (conventional, microwave irradiation and ultrasounds) during the aging step (Chimentao *et al.*, 2007). The crystallinity of the precipitated hydrotalcite is a property that can be increased further by the hydrothermal treatment (Montanari *et al.*, 2010). An effective method is that of microwave irradiation which reduces the time and temperature of crystallization. However, control of synthesis depends on parameters such as molar ratio or the power of the irradiation with microwaves as described in established in a previous work of Rivera *et al.* (2006). Bang and Suslick (2010) between many authors reported the recent advances in nanostructured materials when they recurred the utilization of high intensity ultrasound; the primary physical phenomena associated with ultrasound that are relevant to materials synthesis are acoustic cavitation (implosive collapse of bubbles in a liquid) and nebulization (impinging on a liquid-gas interface) serves as the origin of most sonochemical phenomena in liquids or liquids-solid slurries (Bang *et al.*, 2010) and etoxide-acetylacetonate (Paredes *et al.*, 2015).

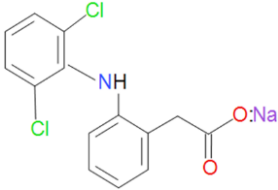
The objective of the present study was to investigate the degradation of DCF by the oxide mixtures of hydrotalcites (Zn/Al, Zn/Al-La, Zn-Mg/Al) and the TiO<sub>2</sub> photocatalysis process in DCF concentration (50 mg L<sup>-1</sup>) in a batch reactor system. The degradation rate was evaluated in term of UV absorbance. The effect of incorporation of lanthum to hydrotalcites in the photocatalytic behavior during the degradation of DCF was studied and discussed.

## 2 Experimental section

### 2.1 Materials and reactives

Aluminum nitrate nonahydrate [Al(NO<sub>3</sub>)<sub>3</sub>·9H<sub>2</sub>O, 98% Sigma Aldrich], zinc nitrate nonahydrate [Zn(NO<sub>3</sub>)<sub>2</sub>·9H<sub>2</sub>O, 98% Sigma Aldrich], magnesium

Table 1. Physicochemical characteristics of diclofenac sodium

Name	Molecular structure	Solubility in water (g/L) *	pKa	Mw (g/mol)	$\lambda_{max}$ (nm)
Diclofenac sodium		2.425	4	318.14	277

\*at 25 °C

nitrate hexahydrate [ $\text{Mg}(\text{NO}_3)_2 \cdot 6\text{H}_2\text{O}$ , 98% Sigma Aldrich], sodium hydroxide [ $\text{NaOH}$ , analytical grade, Sigma-Aldrich], lanthanum nitrate hexahydrate [ $\text{La}(\text{NO}_3)_3 \cdot 6\text{H}_2\text{O}$ , 98 % Sigma Aldrich] were used to prepare layered double hydroxide. Diclofenac sodium salt, CAS No. 15307-76-6, [ $\text{C}_{14}\text{H}_{10}\text{Cl}_2\text{NO}_2\text{Na}$  99.5 % puriss, Sigma Aldrich] was used as obtained in the photocatalytic experiments. Titanium (IV) oxide, anatase powder, 99.8% ( $\text{TiO}_2$ ) was provided by Aldrich. In all experiments, distilled water was used as solvent for the preparation of the freshly prepared solutions.

## 2.2 Preparation of layered double hydroxides

The salts of the nitrated compounds were dissolved in distilled water with metallic molar ratio [ $\text{M}^{2+}/(\text{M}^{3+} + \text{M}^{2+})$ ] of  $x=0.25$ , the mix was called A solution. Sodium hydroxide was dissolved in distilled water using a 1.86 N, it was called B solution. A solution was added drop wise to B solution under vigorous stirring, the pH was adjusted to 9.0 under  $\text{N}_2$  atmosphere. The obtained gel was treated with microwave and ultrasound irradiation. In the case of materials prepared by microwave irradiation, the products were treated hydrothermally in a conventional microwave oven operating at 120 W and 2450 MHz, at a temperature of 80 °C and at atmosphere pressure. In case of ultrasound irradiation, the products were irradiated in an Elma D-78224 cleaner container operating at 2.4 kW and 25 kHz in normal mode. In both methods the irradiation time was 10 minutes to improve their crystallinities. During 4 days ageing the precipitates were filtered and then were washed once with hot distilled water (70°C) to eliminate the alkali metals and nitrate ions until the pH 7, the products were dried at 70 °C for 12 h. These samples were labeled according to Table 2.

Table 2. Identification of samples.

Tag	Metallic molar $x=0.25$	Irradiation time (10 min)
MZ	Zn/Al	Microwave
UZ	Zn/Al	Ultrasound
MZL3	Zn/(Al-3%La)	Microwave
UZL3	Zn/(Al-3%La)	Ultrasound
MZL5	Zn/(Al-5%La)	Microwave
UZL5	Zn/(Al-5%La)	Ultrasound
MMZ	Zn-Mg/Al	Microwave
UMZ	Zn-Mg/Al	Ultrasound
$\text{TiO}_2$	NA	NA

The hydroxaltes were calcined at 500 °C for 4 h in an air flow, in order to obtain mixed oxide base catalyst (Valente *et al.*, 2009; Zhang *et al.*, 2016).

## 2.3 Characterization of LDH and mixed oxides

The powder X-ray diffraction (XRD) patterns were recorded from  $2\theta = 5 - 70$  using Rigaku Miniflex 600 diffractometer using  $\text{Cu-K}\alpha$  radiation operation at 40kV and 15 mA. Specific surface areas of the different mixed oxides were obtained with a Nova 4200e Surface Area & Pore Size Analyzer Instruments using the BET methodology, the pore size distribution was evaluated from the desorption isotherms using the BJH method; the samples were pretreated at 150 °C prior to  $\text{N}_2$  adsorption during 8 h. UV-Vis absorption spectra for the different calcined samples were obtained with a Cary-100 Varian spectrophotometer equipped with an integration sphere. A field emission scanning electron microscope (JSM-7800F) equipped with a microanalysis system by disperse energy was used to obtain SEM images and with EDS detector (Morales 2017).

## 2.4 Catalytic activity

Photocatalytic experiments were carried out at room temperature. A 100 mL vessel was filled in with 50 mL

DCF solutions ( $50 \text{ mg L}^{-1}$ ) and the 50 mg of catalyst at natural pH. UV absorbance analysis were found to be useful for a fast and easy to perform measurement to get preliminary information about the degradation formed during oxidation (Czech *et al.*, 2013). The suspension was mixed for 5 minutes before to start the experiment. The vessel was placed in a photo-reactor illuminated from the 20 W black light fluorescent spiral lamp (127 V) emitting radiation between 365 and 465 nm under continuous magnetic stirring during 6 hours. The same procedure of was carried out following the same procedure of photocatalysis test but with the lamp switched off (blank test, photolysis).

## 2.5 Diclofenac degradation

Changes in the concentration of DCF were monitored by taking samples, using a syringe filter, and analyzing those aliquots using a UV-vis spectrophotometer (model precisely Lambda XLS+Spectrometer, Perkin Elmer). The solution was scanned in the 200-400 nm UV region. The absorbance was measured at the wavelength that correspond to the maximum DCF absorbance in the visible region (277 nm,  $UV_{277}$ ) and this wavelength was adopted for the absorbance measurement (Czech *et al.*, 2013). A calibration curve (which it was previously obtained) was utilized to determine the concentration of DCF in each aliquot (Morales, 2017).

### 2.5.1 Structural elucidation

The spectra were obtained using a micrOTOF-QII mass spectrometer Bruker Daltonics equipped with an electrospray ionization source (ESI). The parameters were set as follows: set capillary 2700 V, nebulizer pressure 0.4 Bar, dry gas flow 4 L/min, dry gas temperature 180 °C. The sample was run in the negative ion polarity mode. The scan range was from 50 to 3000 m/z.

## 2.6 •OH radical determination

Fluorescence spectra of 2-hydroxyterephthalic acid were measured on Spectrofluorophotometer Shimadzu RF-5301PC. The •OH radical generated by the material semiconductor in absence of the diclofenac was evaluated by using terephthalic acid (T.A.) was dissolved in a water /NaOH solution (Mendoza-Damian *et al.*, 2016). Then 200 mg of photocatalyst

was added and the suspension was stirred for 5 min under dark condition. After it was irradiated by black light fluorescent spiral lamp (20 W, 127 V) during 6 hours, and aliquots were taken at different time. Spectrofluorophotometer excited at 315 nm analyzed the fluorescence emission spectra of the irradiated solution.

## 3 Results and discussions

### 3.1 Characterization of materials

The XRD patterns of the samples, shown in Fig 1, exhibit the characteristic reflections of layered double hydroxides (003), (006), (012), (009), (018), (110) and (113) in all the samples, the diffraction peaks matched by the JCPDS card No. 38-0486. For the sample MZ, MZL3 and MZL5 is possible to note two diffractions for the peaks corresponding at  $2\theta = 10.4$  and  $11.4^\circ$  for diffraction (003) and  $2\theta = 20.1$  and  $23^\circ$  for diffraction (006), it could be a mixture for LDH with nitrate and carbonated, because the synthesis was made in atmospheric air (Cavani *et al.* 1991). This double signal was presented only in the samples synthesized with microwave treatment. The crystal size could be calculated from the index Miller (003) and (110), using the Debye-Sherrer equation. Also, as in Figure 3 shows the sample MZ presents additional reflections associated to the ZnO such as characteristic reflections (100), (002) and (101), that are characteristics for LDH with molar metal ratio less than 0.3 (Ramírez *et al.*, 2017). For the sample MZ the most intensive peak can be observed at  $2\theta = 11.4, 23, 34.5, 39.3, 46.6, 60.2$  and  $61.5^\circ$ , which represents the characteristics peaks of hydroxalcite materials (Tzompantzi *et al.*, 2014; Cavani *et al.*, 1991). In the samples MZ and MMZ was possible to observe a characteristic reflection of nitrate ( $\text{NaNO}_3$ ) at  $2\theta = 29.4$ , it was mark with an asterisk (\*). The samples synthesized with ultrasonic treatment presents the characteristic reflections for layered double hydroxides but less defined reflections, that it could be less crystalline materials than the LDH synthesized with microwaves treatment. The others LDH samples with cations with Zn/Al-La and with Mg-Zn/Al presents the typical reflections of hydroxalcites forming a ternary LDH material.

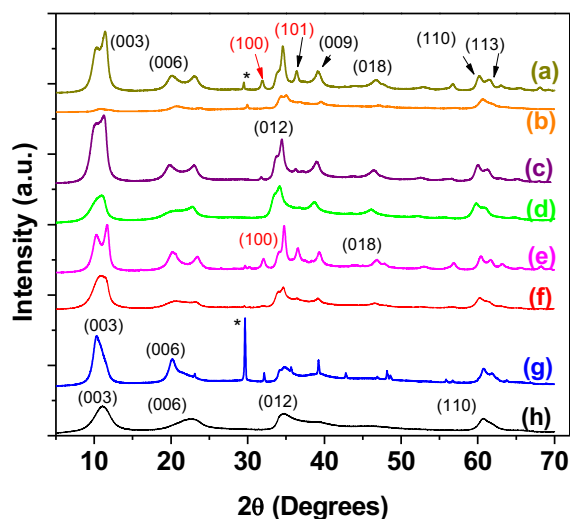


Fig. 1. XRD patterns of MZ(a), UZ (b), MZL3(c), UZL3(d), MZL5(e), UZL5(f), MMZ(g) and UMZ(h).

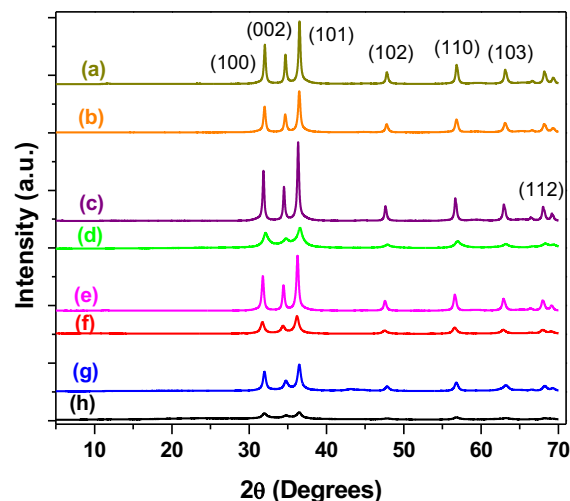


Fig. 2. XRD patterns of calcinated samples cMZ(a), cUZ(b), cMZL3(c), cUZL3(d), cMZL5(e), cUZL5(f), cMMZ(g) and cUMZ(h) at 500 °C.

Figure 2 shows the powder of XRD of the samples calcinated at 500°C during 4 hours, the calcinated samples were prefixed with c minuscule (eg., cMZ) in the tag. The structure of the LDH has been destroyed after calcination; thus, the formation of zinc oxide (zincite) was determined in all the samples; the presence of  $\text{La}_2\text{O}_3$  cannot be observed in the samples with lanthanum (Tzompantzi *et al.*, 2014). The characteristic peaks correspond of index (100), (002), (101), (102), (110), (103) and (112) matched with the ZnO (JCPDS card No. 36-1451), the diffraction lines are in agreement with those calculated by other

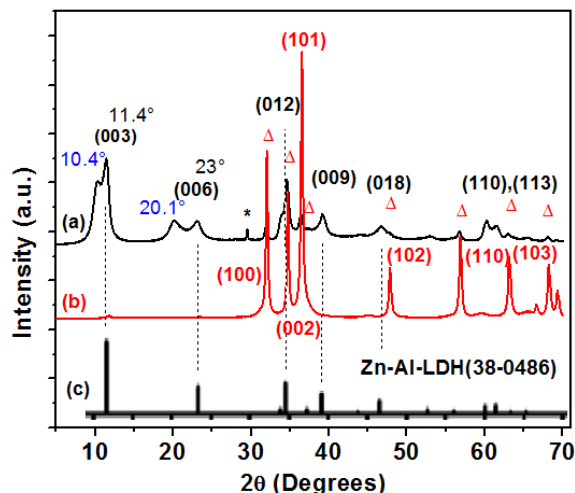


Fig. 3. XRD patterns of LDH MZ(a), cMZ LDH calcined at 500 °C (b), Zn-Al-LDH JCPDS card no. 38-0486 (c).

authors for similar samples (Patzkó *et al.*, 2005). Seftel *et al.* (2008) reported that calcination at 500°C the Al could be present as  $\text{AlO}(\text{OH})$  or the  $\text{Al}^{3+}$  cations could be dispersed in a mostly amorphous phase (Seftel *et al.*, 2008; Zhao *et al.*, 2010).

The treatment at 500 °C is not sufficient for the formation of aluminum oxide crystals (Patzkó *et al.*, 2005). In the diffraction spectrum of the calcined samples (Fig. 2) all the samples using microwaves hydrotreatment show very high intense lines that described the presence of a crystalline ZnO phase than the samples using ultrasound treatment. In all the samples the use of ultrasound treatment affects the crystallinity and the crystal size of the calcined samples.

Figure 4 show the typical nitrogen adsorption-desorption isotherms and their corresponding pore size distribution of the adsorbents. All samples exhibited a type IV isotherm are its hysteresis loop according to the IUPAC classification (Sing *et al.*, 1985) with a H3-type hysteresis loop for the samples cMZ and cMZL5 (treatment with microwaves), which is caused to the presence of slit pores that are coming from the plate like particles giving rise to slit shaped pores. On the other hand, the isotherm of cUZ and cUZL5 showed a H1-type hysteresis loop, where the two branches are almost vertical, which was attributed to capillary condensation and more defined cylindrical pore channels. The adsorption isotherms of the samples showed the monolayer-multilayer adsorption that takes place between the aggregates of platelets particles and the capillary condensation



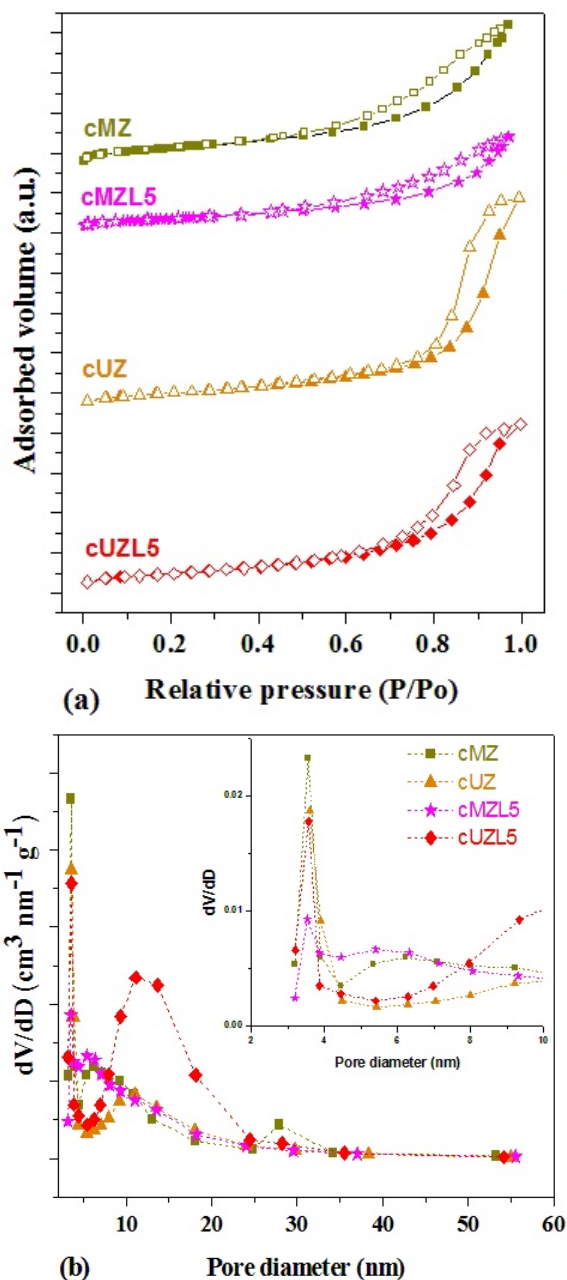


Fig. 4. Nitrogen sorption isotherms at 77 K of mixed oxides. (a) Adsorption isotherms of mixed oxides samples. Closed symbols: adsorption branch, open symbols: desorption branch. (b) BJH Pore size distribution of the samples.

for the characteristics mesoporous materials, but definitely, the isotherms are different for samples with microwave and ultrasound treatment. Longchao Du and Baojun Qu showed that the ultrasound synthesized

hydroxalces have more lattice defects and LDH have

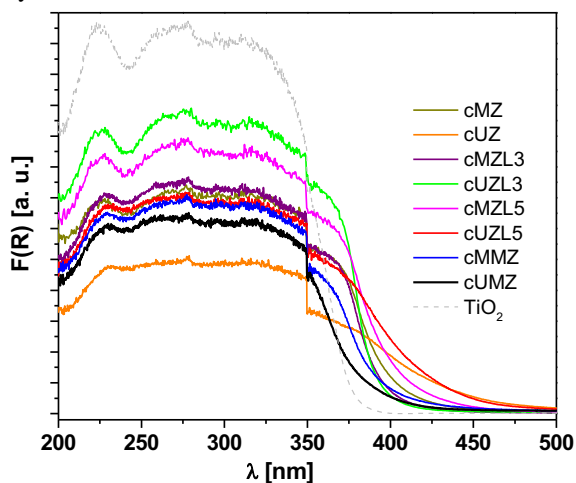


Fig. 5. Difuse reflectance spectra of samples: cMZ (a), cUZ (b), cMZL3 (c), cUMZL3 (d), cMZL5 (e), cUZL5 (f), cMMZ (g) and cUMZ (h).

larger crystal sizes than those prepared by mechanical stirring method. The crystal sizes increase with increasing the reaction temperatures (Longchao *et al.* 2007). The surfaces areas were calculated using the Brunauer-Emmett-Teller (BET) method, whereas the pore size distribution was determined by the Barrett-Joyner-Halenda (BJH) method using the desorption branch of the BJH method indicated that the data can be fitted to the size range of layered materials. The study of textural properties of all the samples have been recorded in the Table 3; the specific surface areas for mixed oxides of Mg-Zn/Al were lower between 14 to 20 m<sup>2</sup>/g and for the mixed oxides of Zn/Al y Zn/Al-La were from 26 and 49 m<sup>2</sup>/g. Based on the observed specific surface areas are independent of the irradiation method. In general, the average pore diameter of the samples synthesized with ultrasound is greater than that obtained with the samples synthesized with microwaves. Paredes *et al.* (2015) considered that the crystallinity, the interlayer distance and specific surface area are dependent on the compensation anion more than the irradiation technique. The results for all the samples showed at the pore size distribution of the diameter BJH and the average pore diameter that the mixed oxides samples were included in the category of mesoporous materials. Figure 5 presents UV-vis diffuse reflectance spectrum of calcined samples and TiO<sub>2</sub>. A wide absorption ranged from 350 to 460 nm was observed for all the samples.

Table 3. Textural properties and band gap values of calcined samples.

Tag	BET (m <sup>2</sup> /g)	Pore diameter BJH (nm)	Pore volume (cm <sup>3</sup> /g)	Average pore diameter (nm)	Band gap (eV)
cMZ	49	3.56	0.077	6.84	2.76
cUZ	30	3.61	0.064	9.15	2.29
cMZL3	35	3.53	0.075	7.01	2.84
cUZL3	34	3.55	0.076	6.93	2.96
cMZL5	26	3.53	0.078	11.59	2.69
cUZL5	41	3.57	0.144	13.56	2.37
cMMZ	14	3.59	0.047	12.87	2.79
cUMZ	20	3.86	0.073	13.48	2.87
TiO <sub>2</sub>	7	3.83	0.008	5.37	3.08

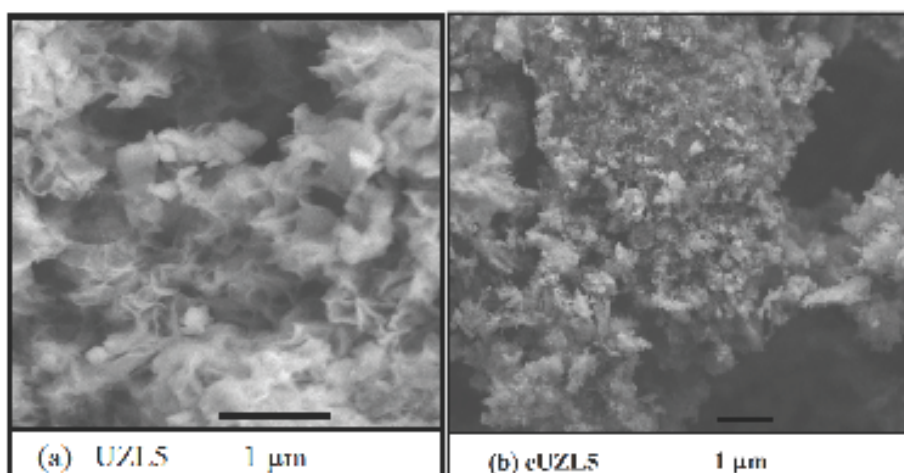


Fig. 6. SEM micrographs for (a) UZL5 (b) cUZL5.

In Table 3 the band gaps energy (E<sub>g</sub>, eV) of the powders of mixed oxides were reported between 2.29 and 2.96 eV, this material was recorded at lower energies and for the TiO<sub>2</sub> was 3.08 eV. In Figure 5 show a shift in visible region for some samples (cUZL5 and cUZ) it could open the possibility of using this new material under irradiation with sunlight.

From SEM observations (see Fig. 6), it shows the hydrotalcite samples as aggregates with morphologies like platelet particles for (a) micrograph of UZL5 sample with 5% of La, the calcination at 500°C produced the collapse of this morphology and large particles rounded edges are observed. Figure 7 shows the elemental mapping images displayed the uniform and homogeneous distribution of O, Zn, Al and La; the metallic relation calculated was  $x=0.249$  and

the weight percent of La was 6.06. The mission of these impurities (wt.% of La) in introducing in LDH allowed states within the forbidden band of energy that enable the radiative transitions and therefore a more promising photocatalytic activity.

### 3.2 Catalytic activity

Several photocatalytic experiments using mixed oxides (calcined LDH) were carried out for the degradation of diclofenac sodium under ultraviolet light. Figure 8 reports the values of C/Co vs. irradiation time for evaluations of photocatalysis in the presence of calcined Zn/Al, Zn-Mg/Al and Zn/Al-La (for 3 and 5 %). The TiO<sub>2</sub> and photolysis (UV) were compared for 50 mgL<sup>-1</sup> initial DCF concentration (Co).

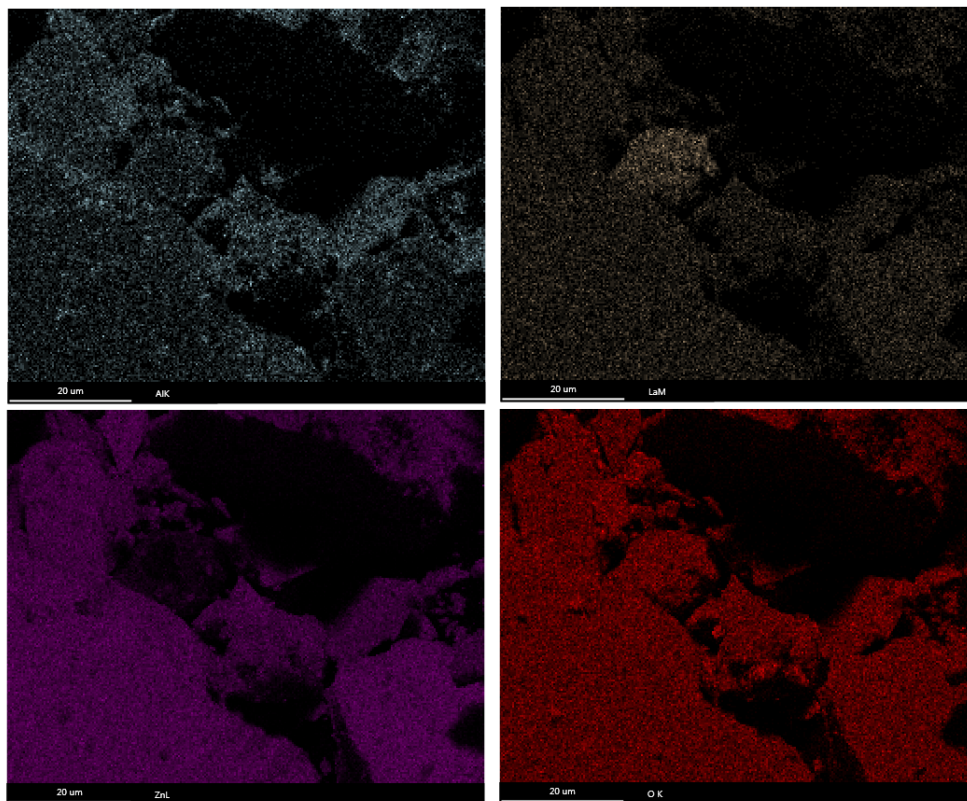


Fig. 7. SEM image for LDH UZL5 sample, EDS mapping images of the O, Zn, Al and La elements.

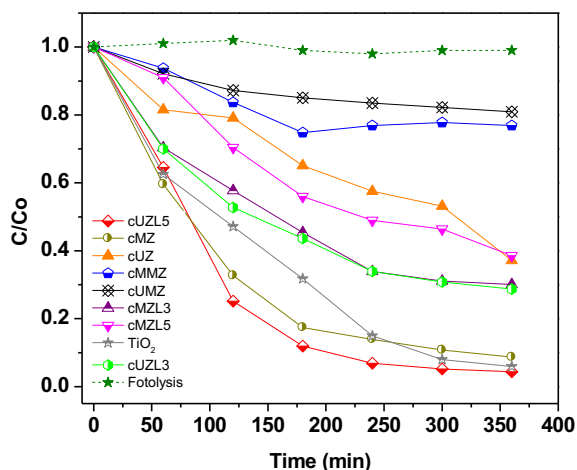


Fig. 8. Photocatalytic behavior of the degradation of DCF in aqueous solution using mixed oxides of Zn/Al, Mg-Zn/Al and Zn/Al-La LDHs under UV light.

All the mixed oxides evaluated showed a degradation response of diclofenac to a greater or lesser extent. This experiment was repeated three

times to ensure consistency of results. The results of one of these three experimental runs are depicted in Figure 8.

First, the results of the photolysis are presented, which indicates that there was no effect by the action of the single ultraviolet light on the study drug. The samples with lower performance were the mixed oxides with Mg/Zn/Al. The samples with mixed oxides with Zn/Al/La in general were those that presented better degradation results of diclofenac. The samples with the highest surface area (49 and 41 m<sup>2</sup>/g) were the two samples that presented the highest performance in the degradation reaching C/Co ratios of 83 and 88% at 180 minutes, being the samples of cMZ and cUZL5, respectively. Experimental results of TiO<sub>2</sub> photocatalytic oxidation of DCF showed the Langmuir-Hinshelwood (L-H) kinetic model (Calza *et al.*, 2006). The disappearance of DCF as well as the mineralization rate depends on several factors including the initial concentration of the target compound, the photocatalyst loading and the irradiation time.



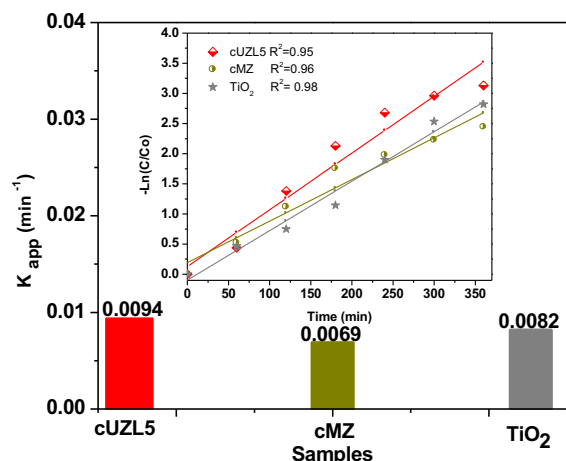


Fig. 9. Apparent rate constants for the photocatalytic degradation of DFC by mixed oxides samples and TiO<sub>2</sub>. Inset: Pseudo-first order kinetics for the photocatalytic degradation of DCF on mixed oxides of LDH and TiO<sub>2</sub>.

Consider the simplest case, DCF decomposing by two or more competing paths, Eq. (1), all elementary reactions (Rizzo *et al.*, 2009).



The rates of change of the all components are given by Eq. (2):

$$-r_A = -\frac{dC_A}{dt} = k_1 C_A + k_2 C_A + k_3 C_A = (k_1 + k_2 + k_3) C_A \quad (2)$$

It would be considered irreversible reactions in parallel, as multiple reactions. First of all, Eq. (2), which is of simple first order, is integrated to give Eq. (3).

$$-\ln \frac{C_A}{C_{A0}} = (k_1 + k_2 + k_3)t \quad (3)$$

When plotted as in Figure 9 inset, the slope is  $k_1 + k_2 + k_3 = K_{app}$  (Levenspiel, 1999). The DFC degradation were fitted to pseudo-first order kinetics (with the obtained linearly dependent coefficients all around 0.95) (Figure 9), in which the value of rate constant ( $K_{app}$ ) is equal to the corresponding slope of the fitting line. The  $K_{app}$  of cUZL5 was 0.0094 min<sup>-1</sup>, which was higher than cMZ and TiO<sub>2</sub>. In Figure 9 the behavior of the samples cUZL5 and cMZ are similar because both of them are mixed oxides

from layer double hydroxides, but the little difference

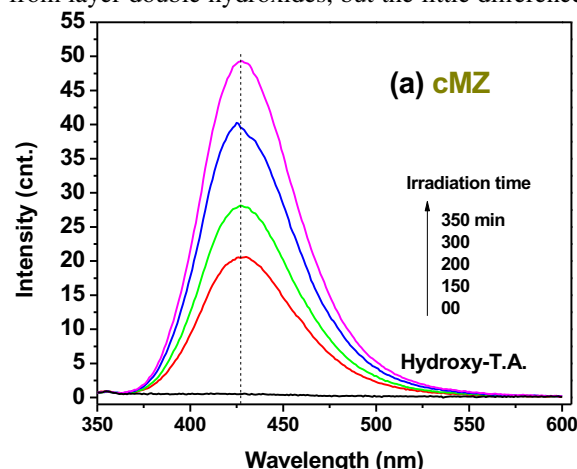


Fig. 10. Fluorescent spectrum of hydroxyl terephthalic acid during the irradiation of the samples cMZ for the selected photocatalyst in the absence of diclofenac.

is their composition. These results implied that the interaction of La and ZnO took an important role in the enhancement of photoactivity.

### 3.3 Formation of •OH radical

To explore the mechanism of diclofenac photocatalytic behavior, the formation of active hydroxyl radicals (•OH) upon irradiation were monitored; it was considered the most important oxidative intermediate in photocatalytic reactions. There was studied the cMZ and the cULZ5 samples, both presented the fluorescence signal associated to the formation of 2-hydroxy terephthalic acid generated by using the samples in absence of diclofenac, both samples presented an increment as time progress during the evaluation. As reference, in the Figure 10, it represents the behavior of the sample cMZ (Mendoza-Damián *et al.*, 2016).

### 3.4 Structural elucidation

In the negative ion mode electrospray mass spectrum of the solution of diclofenac four deprotonated molecular [M-H]<sup>-</sup> ions (m/z values, 310.0047, 294.0089, 250.0191 and 172.9578) were apparent. Table 4 shows the proposed structures for the deprotonated molecular ions [M-H]<sup>-</sup>, with m/z values. The major degradation products produced in the agitation state with UV irradiation of diclofenac in deionized water with the presence of •OH radicals are presented in Figure 11.

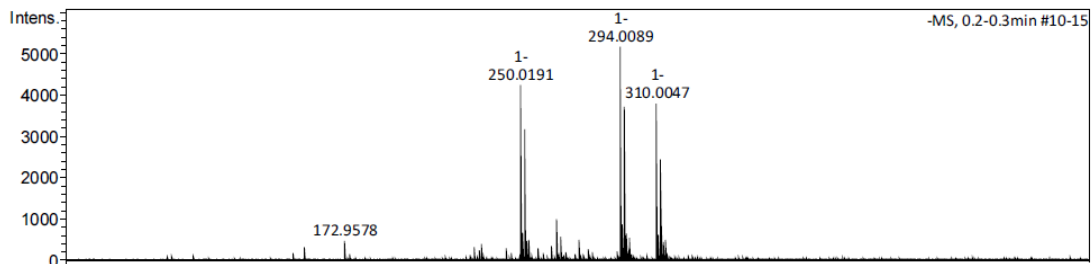


Fig. 11. Analysis of diclofenac sodium ESI-MS spectrum obtained by fragmentation of the  $[M-H]^-$  ion by direct injection of aqueous solution using mixed oxides of Zn/Al-La LDHs under UV light.

Table 4. Molecular ion, molecular formula and molecular structure of the main components of the diclofenac degradation.

Molecular Ion, $[M-H]^-$	Chemical formula	Structural Formula
310.0047	$C_{14}H_{11}Cl_2NO_3$	
294.0089	$C_{14}H_{11}Cl_2NO_2$	
250.0191	$C_{13}H_{11}Cl_2N$	
172.9578	$C_6H_5Cl_2NO$	
172.9578	$C_6H_6O_6$	

The characterization of the degradation products of diclofenac has been previously described (Yu *et al.*, 2013), it was not found a total advanced oxidation process, not a total mineralization was reached in any case.

### 3.5 Mechanisms of reaction

When the samples of study (oxides mixtures of Zn, Al and some of them with La) at 25 °C were irradiated by UV light, the •OH radicals were at first poorly photogenerated giving a low photocatalytic activity and when the time continues it was increasing the photocatalytic activity. It is probable that the presence of La and the ZnO, generate a synergistic effect between them and as a consequence the more e<sup>-</sup>/h<sup>+</sup> pair charge can be photogenerated allowing the formation of more •OH radicals reacting with the diclofenac compounds or with the intermediates products.

## Conclusions

In the present study, the synthesis of layered double hydroxide of Zn/Al, Zn-Mg/Al, Zn/Al-La by microwave thermal and ultrasonic thermal treatment were reported. We confirm that the use of microwave during aging allows us to obtain LDH or hydrotalcites with high crystallinity and the use of ultrasonic treatment allows us to obtain LDH with low crystallinity at the same time of treatment. The Zn/Al, Zn-Mg/Al, Zn/Al-La mixed oxides after calcination of LDH are showed. The nitrogen adsorption-desorption isotherms and the pore size distribution graphics obtained for the mixed oxides show the mesoporosity characteristics. SEM techniques allow us to observe that sample of Zn/Al-La LDH was completely homogeneous. The results obtained in the application of these materials for the photocatalytic degradation of DCF, allow us to propose that, Zn/Al-La mixed oxides are promising materials for a very efficient degradation of diclofenac, reaching 88% at 180 minutes of partial degradation in comparison to the reference TiO<sub>2</sub>, in which the DCF degradation was only 68% at the same time. Based on the behavior of the DCF degradation, the mixed oxides were more active mainly due to the textural properties produced by the synthesis method and the interaction of the Lanthanum in their composition. Product identification was consistent with hydroxylation mechanism, but there was not a

total mineralization, it is possible to degraded products with higher irradiation dose.

### Acknowledgment

The authors are grateful to IPN for the financial support (SIP-20161758 and SIP-20171120), special financial support (ICyTDF/207/2012) and Centro de Nano, Micro y Nanotecnología from IPN by technical support. The technical support of Dr. Elim Albiter and the facilities for the ESIQIE Postgraduate Catalysis Lab are widely acknowledged.

## References

- Andreozzi R., Raffaele M.; Nicklas P. (2003). Pharmaceuticals in STP effluents and their solar photodegradation in aquatic environment. *Chemosphere* 50, 1319-1330.
- Bang J. H.; Suslick K. S. (2010). Applications of ultrasound to the synthesis of nanostructured materials. *Advanced Materials* 22, 1039-1059.
- Bergadá O.; Vicente I.; Salagre P.; Cesteros Y.; Medina F.; Sueiras J. (2007). Microwave effect during aging in the porosity and basic properties of hydrotalcites. *Microporous and Mesoporous Materials* 101, 363-373.
- Calza P.; Sakkas V.A.; Medana C.; Baiocchi C.; Dimou A.; Pelizzetti E.; Albanis T. (2006). Photocatalytic degradation study of diclofenaco over aqueous TiO<sub>2</sub> suspensions. *Applied Catalysis B: Environmental* 67, 197-205.
- Cavani F.; Trifiro F.; Vaccari A. (1991). Hydrotalcite-type anionic clays: preparation, properties and applications. *Catalysis Today* 11, 173-301.
- Chimentao R.; Abelló S.; Medina F.; Llorca J.; Sueiras J.; Cesteros Y.; Salagre P. (2007). Defect-induced strategies for the creation of highly active hydrotalcites in base-catalyzed reactions. *Journal of Catalysis* 252, 249-257.
- Climent M. J.; Corma A.; Iborra S.; Epping K.; Vellty A. (2004). Increasing the basicity and catalytic activity of hydrotalcites by different synthesis procedures. *Journal of Catalysis* 225, 316-326.

- Czech B.; Rubiniowska K. (2013). TiO<sub>2</sub> assisted photocatalytic degradation of diclofenac, metoprolol, estrone and chloramphenicol as endocrine disruptors in water. *Adsorption* 19, 619-630.
- Galmier M.; Bouchon B.; Madelmont J.; Lartigue C. (2005). Identification of degradation products of diclofenac by electrospray ion trap mass spectrometry. *Journal of Pharmaceutical and Biomedical Analysis* 38, 790-796.
- Khan S.; Bahadar S. and Asiri A. (2016). Toward the design of Zn-Al and Zn-Cr LDH wrapped in activate carbon for the solar assisted decoloration of organic dyes. *RSC Advances* 6, 83196-83208.
- Klavarioti M.; Mantzavinos D., Kassinos D. (2009). Removal of residual pharmaceuticals from aqueous systems by advanced oxidation processes. *Environment International* 35, 402-417.
- Levenspiel O. (1999). *Chemical Reaction Engineering*. Third Edition. John Wiley & Sons. Pp 50-52.
- Longchao D. and Baojun Q. (2007). Effects of synthesis conditions on crystal morphological structures and thermal degradation behavior of hydrotalcites and flame retardant and mechanical properties of EVA/hydrotalcite blends. *Polymer composites* 28, 131-138. DOI 10.1002/pc.20279.
- Mahjoubi F.; Khalidi A.; Abdennouri M.; Barka N. (2017). Zn-Al layered double hydroxides intercalated with carbonate, nitrate, chloride and sulphate ions: Synthesis, characterization and dye removal properties. *Journal of Taibah University for Science* 11, 90-100.
- Mendoza-Damian G., Tzompantzi F., Mantilla a., perez-Hernández R., Hernández-Gordillo A. (2016). Improved photocatalytic activity of SnO<sub>2</sub>-ZnAl LDH prepared by one step Sn<sup>4+</sup> incorporation. *Applied Clay Science* 121, 127-136.
- Montanari T.; Sisani M.; Nochetti M. (2010). Zinc- aluminum hydrotalcites as precursors of basic catalysts: Preparation, characterization and study of the activation of methanol. *Catalysis Today* 152, 104-109.
- Morales Z. J. A. (2017). Evaluación de óxidos mixtos provenientes de compuestos tipo hidrotalcita como agentes fotocatalíticos en la degradación del diclofenaco sódico en agua. Tesis de Licenciatura, ESIQIE, Instituto Politécnico Nacional, México.
- Paredes-Carrera S.; Valencia-Martínez R.; Valenzuela-Zapata M.; Sanchez-Ochoa J.; Castro L. (2015). Study of hexavalent chromium sorption by hydrotalcites synthesized using ultrasound vs. microwave irradiation. *Revista Mexicana de Ingeniería Química* 14, 429-436.
- Parida K. M., Mohapatra L. (2012). Carbonate intercalated Zn/Fe layered double hydroxide. A novel photocatalyst for the enhanced photo degradation of azo dyes. *Chemical Engineering Journal* 179, 131-139.
- Parida K.; Mohapatra L.; Baliarsingh N. (2012). Effect of CO<sub>2</sub>+ substitution in the framework of carbonate intercalated Cu/Cr LDH on structural, electronic, optical, and photocatalytic properties. *Journal of Physical Chemistry C* 116, 22417-22424.
- Parida M.; Baliarsingh B.; SairamPatra B.; Das J. (2007). Copperphthalocyanine immobilized Zn/Al LDH as photocatalyst under solar radiation for decolorization of methylene blue. *Journal of Molecular Catalysis A: Chemical* 267, 202-208.
- Patzkó A.; Kun R.; Hornok V.; Dékány I.; Engelhardt T.; Schall N. (2005). ZnAl layer double hydroxides as photocatalyst for oxidation of phenol in aqueous solution. *Colloids and Surfaces A: Physicochemical Engineering Aspects* 265, 64-72.
- Rivera J.A.; Fetter, G.; Bosch, P. (2006). Microwave power effect on hydrotalcite synthesis. *Microporous and Mesoporous Materials* 89, 306-314.
- Rizzo L.; Meric s.; Kassinos D.; Guida M., Belgiorno V. (2009). Degradation of diclofenac by TiO<sub>2</sub> photocatalysis: UV absorbance kinetics and process evaluation through a set of toxicity bioassays. *Water Research* 43, 979-988.
- Seftel E.M.; Popovici E.; Mertens M.; De Witte K.; Van Tendeloo G. (2008). Zn-Al layered double hydroxides: synthesis, characterization



- and photocatalytic application. *Microporous and Mesoporous Materials* 113, 296-304.
- Sing K.; Everett D.; Haul R.; Moscou L.; Pierotti R.; Rouquérol J.; Siemieniowska (1985). T. Reporting physisorption data for gas/solid systems with special reference to the determination of surface area and porosity. *Pure & Applied Chemistry* 57, 603-619.
- Tzompantzi F.; Mendoza-Damián G.; Rico J.L.; Mantilla A. (2014). Enhanced photoactivity for the phenol mineralization on ZnAlLa mixed oxides prepared from calcined LDHs. *Catalysis Today* 220-222, 56-60.
- Valente J.S.; Tzompantzi F.; Prince J.; Cortez J.; Gomez R. (2009). Adsorption and photocatalytic degradation of phenol and 2,4 dichlorophenoxyacetic acid by Mg-Zn-Al layered double hydroxides. *Applied Catalysis B: Environmental* 90, 330-338.
- Yu H., Nie E., Xu J. Cooper W., Song W. (2013). Degradation of diclofenac by advanced oxidation and reduction processes: Kinetic studies, degradation pathways and toxicity assessments. *Water Research* 47, 1909-1918.
- Zhang L.; Xiong Z.; Burt R.; Zhao X.S. (2016). Uptake and degradation of orange II by zinc aluminum layered double oxides. *Journal of Colloid Interface Science* 1-469, 224-230.
- Zhao X.; Zhang F.; Xu S.; Evans D.G.; Duan X. (2010). From layered double hydroxides to ZnO based mixed metal oxides by thermal decompositions: transformation mechanism and UV-blocking properties of the product. *Chemical Materials* 22, 3933-3942.